Molecular Simulation

ISSN: 0892-7022 (Print) 1029-0435 (Online) Journal homepage: http://www.tandfonline.com/loi/gmos20

Band gap and electronic properties of molybdenum disulphide under strain engineering: density functional theory calculations

Chuong V. Nguyen, Victor V. Ilyasov, Hieu V. Nguyen & Hieu N. Nguyen

To cite this article: Chuong V. Nguyen, Victor V. Ilyasov, Hieu V. Nguyen & Hieu N. Nguyen (2016): Band gap and electronic properties of molybdenum disulphide under strain engineering: density functional theory calculations, Molecular Simulation, DOI: 10.1080/08927022.2016.1233549

To link to this article: http://dx.doi.org/10.1080/08927022.2016.1233549

Published online: 28 Sep 2016.

Submit your article to this journal

Article views: 7

View related articles

View Crossmark data

Full Terms & Conditions of access and use can be found at
http://www.tandfonline.com/action/journalInformation?journalCode=gmos20

Download by: [Mount Royal University] **Date:** 03 October 2016, At: 09:38

MOLECULAR SIMULATION, 2016
http://dx.doi.org/10.1080/08927022.2016.1233549

Band gap and electronic properties of molybdenum disulphide under strain engineering: density functional theory calculations

Chuong V. Nguyen[a,b], Victor V. Ilyasov[c], Hieu V. Nguyen[d] and Hieu N. Nguyen[a]

[a]Institute of Research and Development, Duy Tan University, Da Nang, Vietnam; [b]Department of Materials Science and Engineering, Le Quy Don Technical University, Hanoi, Vietnam; [c]Physics Department, Don State Technical University, Rostov on Don, Russia; [d]Physics Department, Da Nang University of Education, Da Nang, Vietnam

ABSTRACT

In this paper, we study the effect of uniaxial and biaxial strain on the structural and electronic properties of MoS_2 monolayers by first-principle calculations based on density functional theory. Our calculations show that the bond length between Mo and S atoms $d_{\mathrm{Mo-S}}$ depends linearly on the strain. At the equilibrium state, MoS_2 has a direct band gap of 1.72 eV opening at the K-point. However, an indirect–direct band gap transition has been found in MoS_2 monolayer when the strain is introduced. MoS_2 becomes a semiconductor with an indirect band gap when the uniaxial strain $\varepsilon_x \geq 1\%$ or the biaxial strain $\varepsilon_{xy} \geq 1\%$. Under biaxial strain, a metal–semiconductor transition occurs at 18% of elongation. The indirect character and phase transition will largely constrain application of MoS_2 monolayer to electronic and optical devices.

ARTICLE HISTORY
Received 11 April 2016
Accepted 21 August 2016

KEYWORDS
Molybdenum disulphide; strain engineering; electronic property; density functional theory

1. Introduction

Molybdenum disulphide (MoS_2) is currently one of most interesting materials for applications in nano-electronic devices due to its unique mechanical, electronic and optical properties.[1,2] It is a single atomic layer, which is similar to graphite. It is well known that the van der Waals (vdW) interaction between MoS_2 layers is weak, therefore we can easily obtain the monolayer MoS_2. It is a typical example of layered transition-metal di-chalcogenides family, which has been both theoretically and experimentally studied in recent years.[3,4] Together with the large energy band gap, the high carrier mobility [5,6] makes MoS_2 well suited for applications in transistors,[7] photo-detectors,[8] and memory devices.[9]

Bulk MoS_2 is known as semiconductor with indirect band gap of 1.23 eV.[10] While the bulk material has an indirect gap and the monolayer MoS_2 is a direct semiconductor with band gap of 1.80 eV [10] opening at the K point. Monolayer MoS_2 has been successfully fabricated through different methods.[11–14]

Electronic properties of MoS_2 are very sensitive to structural perfection [15] and they can be controlled and tuned by chemical treatment, nanopatterning, functionalisation, nanocatalyst [16] through adatom adsorption, applied external electric field or strain engineering.[17–22] In recent years, many works have been focused on the strain engineering of MoS_2 from both the experimental [10,23] and theoretical [24–26] to explore the effect of strain in-plane on physical properties of MoS_2.[1,2] Besides, effect of strain (out-of-plane direction) on electronic properties of MoS_2 monolayer has been both theoretically and experimentally studied by Peña-Álvarez et al. [27].

In present work, with the use of density functional theory (DFT) computations, we systematically investigated effect of uniaxial and biaxial strain engineering on the band gaps and electronic properties of monolayer MoS_2. The uniaxial and biaxial strain is located in-plane (*xy* plane) in our all calculations. The direct-to-indirect band gaps and semiconductor-to-metal transition are observed in monolayer MoS_2 when strain applied in our calculation. Our calculations show that the band gaps of monolayer MoS_2 can be reduced to zero when the biaxial strain was introduced. Our computational results provide many useful ways for applications of monolayer MoS_2 in nanoelectromechanical and optoelectronic devices.

2. Computational method and model

In this work, we calculate the structural and electronic properties of the monolayer MoS_2 by DFT using accurate frozen-core full-potential projector augmented-wave pseudopotentials,[28, 29] as implemented in the Quantum Espresso code.[30] We use the generalised gradient approximation (GGA) with the parametrisation of Perdew-Burke–Ernzerhof (PBE). This approach has been successful in investigating nanosystems based on graphene.[31] The electronic wavefunctions were described by plane-wave basis sets with a kinetic energy cut-off of 30 Ry, and the energy cut-off for the charge density was set to 300 Ry. The structure is fully relaxed with an energy convergence of 10^{-6} eV and a force convergence of 0.01 eV/Å. The Brillouin-zone integration is carried out by a $18 \times 18 \times 1$ k-mesh according to the Monkhorst-Pack scheme. For the different layers of the MoS_2, the supercells are constructed with a vacuum space of 20 Å along the *z*-direction. The strain is simulated by setting the lattice parameter to a fixed larger value and relaxing the atomic positions. The magnitude of strain is defined as: $\varepsilon = (a - a_0)/a_0$, where a_0 and a are the lattice parameters of the unstrained and strained systems, respectively.

CONTACT Chuong V. Nguyen chuongngnguyen11@gmail.com
© 2016 Informa UK Limited, trading as Taylor & Francis Group

The hexagonal structure of MoS_2 bulk with the lattice parameters a = 3.16 Å, and c/a ratio of 3.89 was taken as starting point for the geometry relaxation. After the relaxation, our calculations show that the lattice parameter for the bulk MoS_2 is 3.18 Å, and c/a ratio is 3.85. The calculated energy band gap for the optimised structure of bulk MoS_2 is 1.22 eV. This result is in good agreement with the experimental value (1.23 eV).[10] We then built structures of MoS_2 monolayer, starting with the lattice parameters of the bulk relaxed MoS_2.

3. Results and discussion

To study the effect of strain on the band gap and the electronic properties of graphene-like MoS_2 monolayer, the geometry of monolayer MoS_2 is relaxed and optimised by dispersion-corrected density functional theory (DFT-D2). The lattice constant a_0 of MoS_2 monolayer after relaxation is 3.18 Å, which is in good agreement with 3.20 Åusing GGA method,[32] and also finds very good agreement with experimental value of 3.16 Å.[33] The bond distance between Mo and S atoms is d_{Mo-S} = 2.42 Å, which is in good agreement with GGA calculations (2.42 Å),[34] and experimental studies (2.41 Å).[33] The relaxed bond angle S–Mo–S in MoS_2 monolayer is $\theta = 81.04°$. Available data for bond angle by Kumar and Ahluwalia [35] is 81.73° (80.88°) using LDA (GGA).

Using DFT-D2 calculations, we show that the band gap of MoS_2 monolayer is 1.72 eV which is very close to recent DFT calculations,[24,36–39] but smaller than that measured using complementary techniques of optical absorption, photoluminescence and photoconductivity (1.80 eV) of monolayer thick MoS_2.[10] The band gap problem can be addressed more accurately by the GW approximation [32,34] which has not been carried out in this paper. However, this trend is not generalized, and depends on the material considered. For example, based on the many-body GW method, Actaca et al. [32,34] showed that the band gap is higher than 2.78 eV. Therefore, we believe that our choice of the dispersion-corrected DFT for the MoS_2 structure is appropriate, and a new idea of the trends can be obtained from our results.

The strained cell is modelled by stretching of hexagonal ring in the x- or xy-directions. The top and side views of the generalised structure of semiconducting MoS_2 monolayer with hexagonal symmetry and its strain directions are illustrated in Figure 1. Strain engineering is applied in two different ways: uniaxial expansion of monolayer in the x direction, and biaxial expansion in the xy direction. The components of strain along x and xy directions are noted as ε_x and ε_{xy}, respectively. The strains are evaluated as the lattice stretching percentage. A wide range of strain along (up to 18%) both directions has been employed in the present study.

Figure 2(a) shows the total energy of semiconducting MoS_2 monolayer as function of strain engineering ε_x and ε_{xy}. The effect of the uniaxial and biaxial strain on the bond length d_{Mo-S} is also shown in Figure 2(b),(c). At the equilibrium (unstrained), the total energy of the semiconducting MoS_2 monolayer is minimal. The linear dependence of the total energy on uniaxial strain is described by a parabolic shape. Figure 2(a) also shows that the total energy of MoS_2 monolayer under strain along the xy direction is higher than that along the x direction. When the strain along the xy direction is applied, the semiconducting MoS_2 monolayer turns out to be less stable than under the strain along the x direction.

In the each layer of MoS_2, we denote the bond length between Mo atom and three nearest neighbour S atoms (S1, S2, and S3) by d_1, d_2 and d_3, respectively. Our calculations show that, at the equilibrium state, these bond lengths are $d_1 = d_2 = d_3 =$ 2.42 Å. This values coincide with results of previous theoretical [34,35,40–42] and experimental [33] studies. As shown in Figure 2(b), the bond lengths d_1 along the x direction (d_1^x) do not depend on the strain, but other quantities depend strongly on the uniaxial strain, especially d_2^x and d_3^x.

Dependence of the band gap of MoS_2 monolayer on bond lengthe S–Mo (d_1) and bond angle S–Mo–S (θ) under applied strain is illustrated in Figure 3. One can shows that, the closure of S–Mo–S angle is associated with the metallisation of this compound. This result is in good agreement with previous study.[27] Figure 4 shows the dependence of the band gap of MoS_2 monolayer on strain engineering along x and xy directions. At the equilibrium state, MoS_2 monolayer is a semiconductor. A direct band gap of 1.72 eV opens at the K-point as shown in Figure 4(a). Our result is in good agreement with previous calculations.[24,36–39]

In Figure 4(a), we can see that the difference in energy between the highest subband of the valence band at K-point (highest energy) and Γ-point, $\Delta E_{HVB}^{K\Gamma}$, is negligible. The $\Delta E_{HVB}^{K\Gamma}$ is only 0.04 eV. This difference in energy will easily lead to a transformation from a direct to an indirect semiconductor in monolayer MoS_2.

We now apply uniaxial along the x direction in monolayer MoS_2. Let us focus on the highest subband in the valence band of MoS_2. Our calculations show that the $\Delta E_{HVB}^{K\Gamma} = E_{HVB}^{K} - E_{HVB}^{\Gamma}$ is equal to -0.8 meV at $\varepsilon_x = 1\%$, where E_{HVB}^{K} and E_{HVB}^{Γ} are the energy at the K point and Γ point in the highest subband of the valence band. It means that the MoS_2 monolayer becomes an indirect semiconductor when $\varepsilon_x \geq 1\%$ and the highest energy of the valence band is in the Γ point of the reciprocal lattice. This energy is strongly dependent on uniaxial strain as shown in Figure 4. Note that the bottom of the conduction band is always located at the K point. The dependence of the indirect band gap of MoS_2 on the ε_x is shown in Figure 4(f) and the transformation from direct to indirect semiconductor of MoS_2 as a result of uniaxial strain is shown in Figure 5.

Figure 4 shows the electronic band gap of MoS_2 monolayer versus the Mo-S distance d_1 and S–Mo–S angle θ.

Similarly, our calculations show that MoS_2 becomes a semiconductor with an indirect band gap when the biaxial strain $\varepsilon_{xy} \geq 1\%$ is introduced. Both under uniaxial strain ε_x and ε_{xy}, the band gap is decreasing in elongation variable. The dependence of the band gap on the strain can be described as a part of a hyperbola as shown in Figure 4(f). This behaviour should be attributed to the change in the atomic orbital composition of the associated crystal wavefunctions at VBM and CBM under various strain values. Investigating the details of these changes in the orbital composition of crystal wavefunctions requires further study and is beyond the scope of the current work. In the case of biaxial strain, the band gap vanishes at $\varepsilon_{xy} = 18\%$. The metal–semiconductor phase transition occurs in MoS_2 due

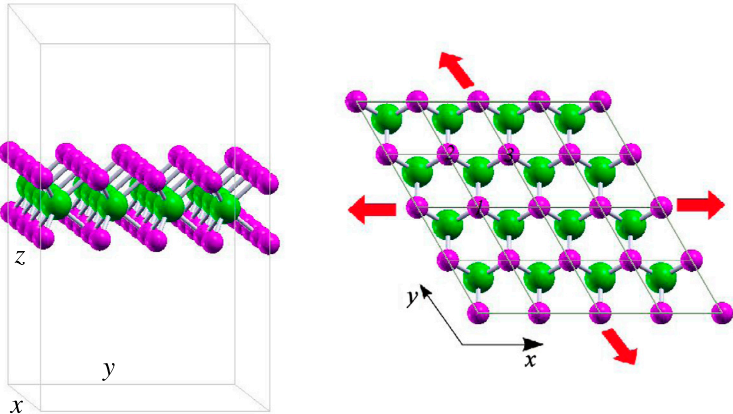

Figure 1. (Colour online) The side view and top view of the graphene-like MoS_2 monolayer. The purple and green stand for the S– and Mo–atoms, respectively.

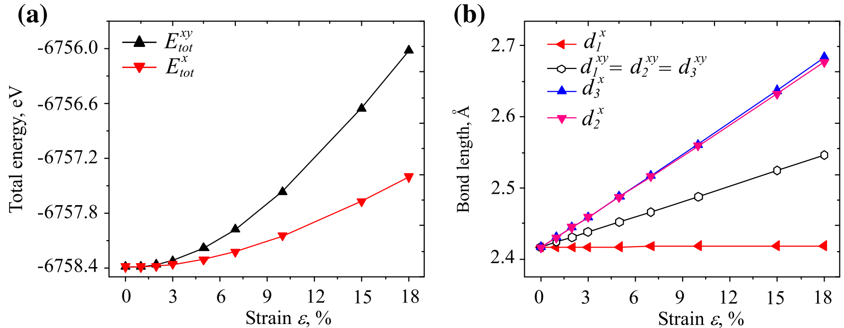

Figure 2. (Colour online) The total energy (a) and bond length (b) as a function of uniaxial and biaxial tensile strain along *x*- and *xy* directions.

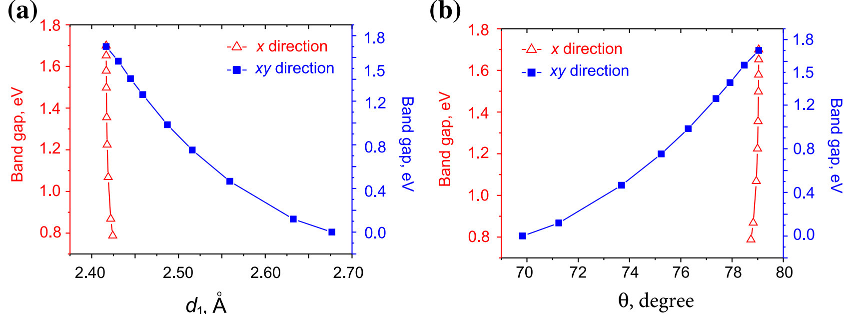

Figure 3. (Colour online) The band gap of MoS_2 monolayer as a function of bond length S–Mo (d_1) (a) and bond angle S–Mo–S (θ) (b). The red vertical axis (left) and blue vertical axis (right) refer to the band gap of MoS_2 under uniaxial in-plane strain along the *x*-direction, and on biaxial in-plane strain along the *xy*-direction, respectively.

to the biaxial strain. The MoS_2 under biaxial strain ε_{xy} is an interesting case. It is a semiconductor with a direct band gap when $0 < \varepsilon_{xy} < 1\%$ and becomes a semiconductor with an indirect band gap when $1\% < \varepsilon_{xy} < 18\%$. Especially, when $\varepsilon_{xy} > 18\%$, the MoS_2 monolayer is metallic. These results are interesting. Not only the band gap of monolayer MoS_2 can be tuned by strain engineering, but also the direct–indirect and semiconductor–metal transitions are tuned. In addition, we also calculate the band gap of MoS_2 monolayer under compressive strain. Our calculations show that, the band gap of MoS_2 monolayer decreases when the compressive strain changes from −5 % to −10 %. The indirect to direct band gap is also observed at the compressive strain of −1 %. The band gap of MoS_2 monolayer under biaxial compressive strain of −1 %, −5 %, and −10 % is 1.76 eV, 1.66 eV, and 1.42 eV, respectively. While, the band gap of MoS_2 monolayer under uniaxial compressive strain of −1 %, −5 %, and −10 % is 1.73 eV, 1.68 eV, and 1.58 eV, respectively.

Figure 5 shows the partial density of states (PDOS) of Mo-*d*, S-*p* and S-*s* orbitals at the equilibrium state and under strain. We can see that at the equilibrium Figure 5(a), the bottom of the conduction band is mainly contributed to by Mo-*d* orbitals, while the top of the valence band is contributed to by Mo-*d* and S-*p* orbitals. Mo-*d* and S-*p* orbitals are together hybridised at the top of the valence band. It means that a strong bonding exists between Mo and S atoms. At the equilibrium, the PDOS of Mo4*d* and S3*p* are almost the same in the energy range

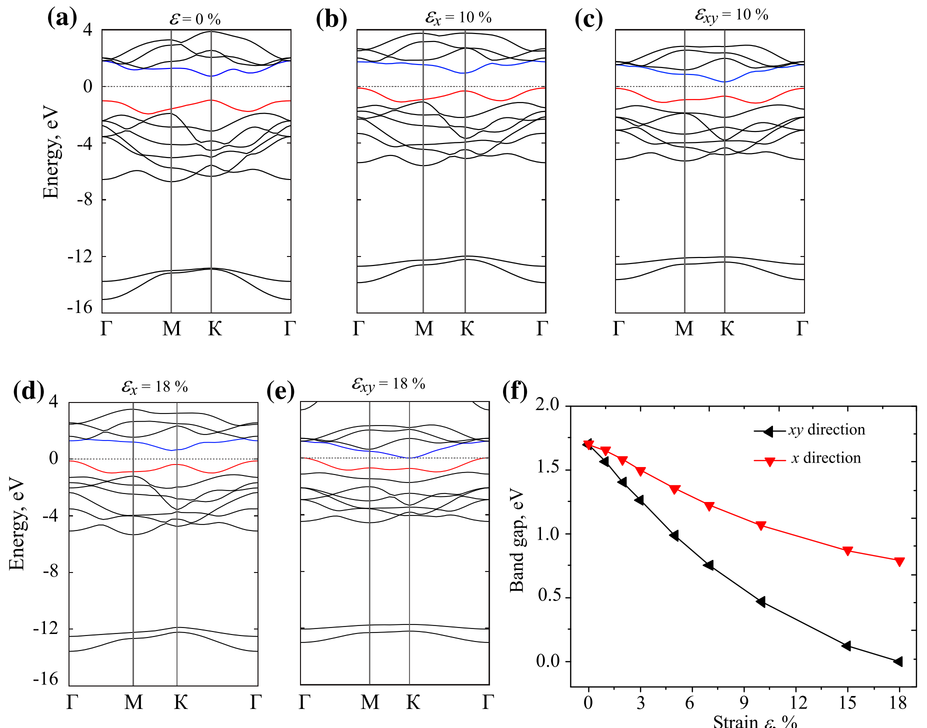

Figure 4. (Colour online) Electronic band structure of MoS_2 monolayer at the equilibrium state (a) and under strain (b, c, d, e). (f) Dependence of band gap of MoS_2 monolayer on strain. The blue and red lines in the band structure refer to the lowest subband of the conduction band and the highest subband of the valence band, respectively.

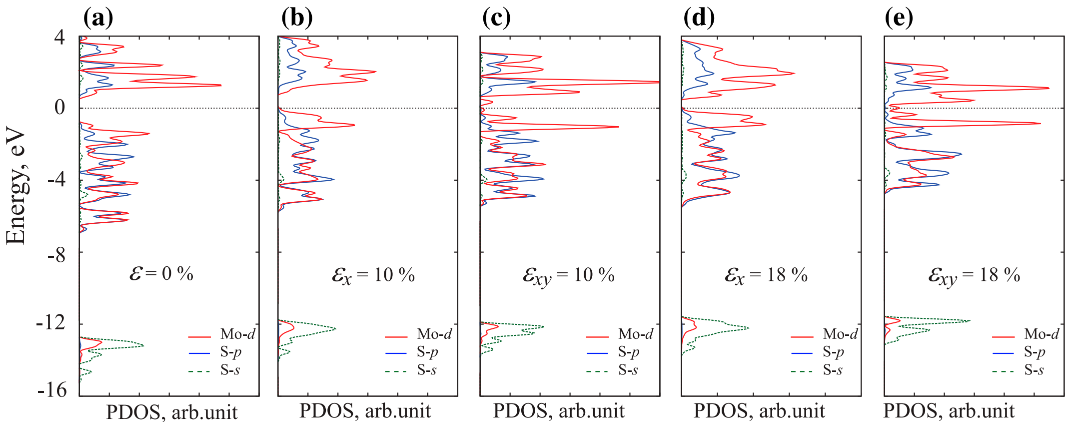

Figure 5. (Colour online) The projected density of states of Mo-d, S-p and S-s orbitals at the equilibrium state (a) and under strain (b)–(e). The horizontal dashed lines refer to the Fermi level.

from −6 to −1 eV. The Mo4d and S3p orbitals share paired electrons. The chemical bonds between Mo atom and six nearest neighbour S atoms in monolayer MoS_2 are covalent bonds. In spite of covalent bonds between S and Mo atoms, charge offset occurs because of difference in electronegativity. This deffence leads the change in the electronic oribitals of Mo and S atoms. The mirror symmetrical bonding configuration in the tri-layer S–Mo–S system results in a weak π bond-like interaction. The weak interaction is very sensitive to the strain, resulting in the changed band structure under strain.

Figure 5 illustrates the projected density states (PDOS) of Mo-d, S-p and S-s orbitals at different strain strengths. We can see that in the range from −1 to 0 eV (the Fermi level), the PDOS depends dramatically on the uniaxial strain (see Figure 5(b),(c)). In Figure 5(e) we show the PDOS of Mo-d, S-p and S-s orbitals at $\varepsilon_{xy} = 18\%$. It is clear that at $\varepsilon_{xy} = 18\%$ MoS_2 is metallic. The indirect character and the strongly dependence of band gap on strain in monolayer MoS_2 can open many ways for applications of MoS_2 in electronic and optical devices.[43]

The PDOS of Mo4d orbitals changes more significant than that of S3p orbital in both cases of uniaxial and biaxial strain. We can see that in the range from −2 to 0 eV (the Fermi level), at 18% of the biaxial strain, the PDOS of Mo4d and S3p are close to zero, resulting in a semiconductor–metal transition in

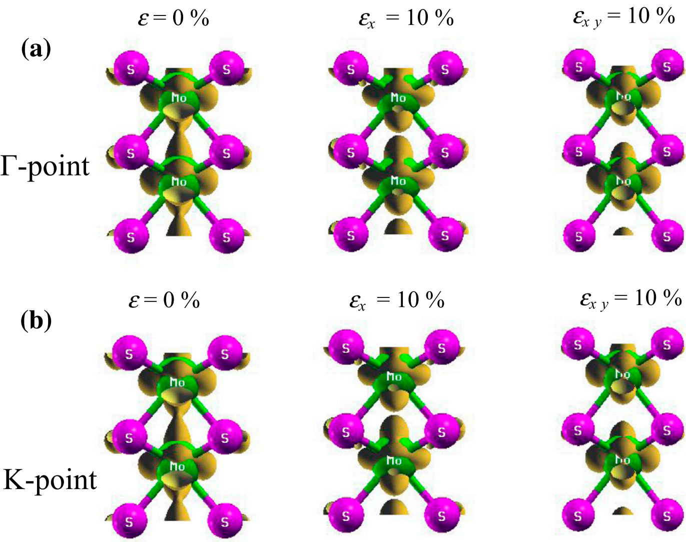

Figure 6. (Colour online) Isosurface plot of the charge density (n) of monolayer MoS_2 (side view) corresponding to the valence band maximum under strain at the Γ- and K- point. The isosurface value was taken as 0.005 eV/Å.

monolayer MoS_2. In Figure 6, we show the isosurfaces of the valence band maximum at the Γ- and K-points with unstrained and strained states. It shows that the valence band maximum at Γ- and K-point is mainly of d_z^2 and p_z orbitals for Mo and S atoms, respectively. In comparison to the unstrained case, when the biaxial strain has been introduced, the isosurface of the valence band maximum changes more significantly than in the case of the uniaxial strain. This is the reason leading to the semiconductor–metal transition at $\varepsilon_{xy} = 18\%$. The indirect nature also can be seem in Figure 5. It shows that the CBM is still at the K point, while the VBM is moved to the Γ point. Hence, the value degeneracy for both VBM and CBM is equal to two in a relaxed structure, whereas the VBM is singly degenerate.

4. Conclusion

In this paper, we investigated the structural properties and electronic states of monolayer MoS_2 under uniaxial/biaxial strain using DFT. We have seen that the mechanical strains reduce the band gap of semiconducting monolayer MoS_2 causing an direct-to-indirect band gap and a semi-conductor-to-metal transition. Our calculations demonstrated that the semiconductor–metal transition occurs in monolayer MoS_2 under the biaxial strain of $\varepsilon_{xy} = 18\%$. The appearance of a phase transition in the monolayer MoS_2 opens many ways for applications in nano-electronmechanical devices based on monolayer MoS_2.

Disclosure statement

No potential conflict of interest was reported by the authors.

ORCiD

Chuong V. Nguyen http://orcid.org/0000-0003-4109-7630
Hieu N. Nguyen http://orcid.org/0000-0001-5721-960X

References

[1] Chhowalla M, Shin HS, Eda G, et al. The chemistry of two-dimensional layered transition metal dichalcogenide nanosheets. Nat. Chem. 2013;5:263–275.
[2] Van der Zande AM, Huang PY, Chenet DA, et al. Grains and grain boundaries in highly crystalline monolayer molybdenum disulphide. Nat. Mater. 2013;12:554–561.
[3] Cappelluti E, Roldan R, Silva-Guillen JA, et al. Tight-binding model and directgap/indirect-gap transition in single-layer and multilayer MoS_2. Phys. Rev. B. 2013;88:075409.
[4] Kaasbjerg K, Thygesen KS, Jacobsen KW. Phonon-limited mobility in n-type single-layer MoS_2 from first principles. Phys. Rev. B. 2012;85:115317.
[5] Baugher BWH, Churchill HOH, Yang Y, et al. Intrinsic electronic transport properties of high-quality monolayer and bilayer MoS_2. Nano Lett. 2013;13:4212–4216.
[6] Radisavljevic B, Kis A. Mobility engineering and a metal-insulator transition in monolayer MoS_2. Nat. Mater. 2013;12:815–820.
[7] Lee G-H, Yu Y-J, Cui X, et al. Flexible and transparent MoS_2 field effect transistors on hexagonal boron nitride-graphene heterostructures. ACS Nano. 2013;7:7931–7936.
[8] Britnell L, Ribeiro RM, Eckmann A, et al. Strong light-matter interactions in heterostructures of atomically thin films. Science. 2013;340:1311–1314.
[9] Sup Choi M, Lee G-H, Yu Y-J, et al. Controlled charge trapping by molybdenum disulphide and graphene in ultrathin heterostructured memory devices. Nat. Commun. 2013;4:1624–1630.
[10] Mak KF, Lee C, Hone J, et al. Atomically thin MoS_2: a new direct-gap semiconductor. Phys. Rev. Lett. 2010;105:136805–136808.
[11] Kim D, Sun D, Lu W, et al. Toward the growth of an aligned single-layer MoS_2 film. Langmuir. 2011;27:11650–11653.
[12] Ganatra R, Zhang Q. Few-layer MoS_2: a promising layered semiconductor. ACS Nano. 2014;8:4074–4099.
[13] Novoselov KS, Jiang D, Schedin F, et al. Two-dimensional atomic crystals. Proceedings of the National Academy of Sciences of the United States of America. 2005;102:10451–10453.
[14] Coleman JN, Lotya M, ONeill A., et al. Two dimensional nanosheets produced by liquid exfoliation of layered materials. Science. 2011;331:568–571.
[15] Hong J, Hu Z, Probert M, et al. Exploring atomic defects in molybdenum disulphide monolayers. Nat. Commun. 2015;6:6293–6300.

[16] Liao T, Sun Z, Sun C, et al. Electronic coupling and catalytic effect on H_2 evolution of MoS_2/graphene nanocatalyst. Sci. Rep. 2014;4: 6256–6262.
[17] Xu W-B, Huang B-J, Li P, et al. The electronic structure and optical properties of Mn and B, C, N co-doped MoS_2 monolayers. Nanoscale Res. Lett. 2014;9:554–560.
[18] Yue Q, Shao Z, Chang S, et al. Adsorption of gas molecules on monolayer MoS_2 and effect of applied electric field. Nanoscale Res. Lett. 2013;8:425–431.
[19] Li X, Wu S, Zhou S, et al. Structural and electronic properties of germanene/MoS_2 monolayer and silicene/MoS_2 monolayer superlattices. Nanoscale Res. Lett. 2014;9:110–118.
[20] Lu S-C, Leburton J-P. Electronic structures of defects and magnetic impurities in MoS_2 monolayers. Nanoscale Res. Lett. 2014;9: 676–684.
[21] Lu P, Wu X, Guo W, et al. Strain-dependent electronic and magnetic properties of MoS_2 monolayer, bilayer, nanoribbons and nanotubes. Phys. Chem. Chem. Phys. 2012;14:13035–13040.
[22] Conley HJ, Wang B, Ziegler JI, et al. Bandgap engineering of strained monolayer and bilayer MoS_2. Nano Lett. 2013;13:3626–3630.
[23] Han S, Kwon H, Kim SK, et al. Band-gap transition induced by interlayer van der Waals interaction in MoS_2. Phys. Rev. B. 2011;84:045409–045412.
[24] Lebegue S, Eriksson O. Electronic structure of two-dimensional crystals from ab initio theory. Phys. Rev. B. 2009;79:115409–115412.
[25] Li T, Galli G. Electronic properties of MoS_2 nanoparticles. J. Phys. Chem. C. 2007;111:16192–16196.
[26] Ataca C, Topsakal M, Aktrk E, et al. A comparative study of lattice dynamics of three and two-dimensional MoS_2. J. Phys. Chem. C. 2011;115:16354–16361.
[27] Peña-Álvarez M, del Corro E, Morales-García A. et al. Single layer molybdenum disulfide under direct out-of-plane compression: low-stress band-gap engineering. Nano Lett. 2015;15:3139–3146.
[28] Blöchl PE. Projector augmented-wave method. Phys. Rev. B. 1994;50:17953–17979.
[29] Kresse G, Joubert D. From ultrasoft pseudo potentials to the projector augmented-wave method. Phys. Rev. B. 1999;59:1758–1775.
[30] Giannozzi P, Baroni S, Bonini N, et al. Quantum espresso: a modular and open-source software project for quantum simulations of materials. J. Phys.: Condens. Matter. 2009;21:395502–395520.
[31] Nguyen CV. IIyasov, V.V., Nguyen, H.N. Tuning the electronic properties of armchair graphene nanoribbons by strain engineering. Phys. Scr. 2015;90:015802–015808.
[32] Ataca C, Ciraci S. Functionalization of single-layer MoS_2 honeycomb structures. J. Phys. Chem. C. 2011;115:13303–13311.
[33] Wilson J, Yoffe A. The transition metal dichalcogenides discussion and interpretation of the observed optical, electrical and structural properties. Adv. Phys. 1969;18:193–335.
[34] Ataca C, Şahin H, Aktrk E. et al. Mechanical and electronic properties of MoS_2 nanoribbons and their defects. J. Phys. Chem. C. 2011;115:3934–3941.
[35] Kumar A, Ahluwalia P. A first principle comparative study of electronic and optical properties of 1H-MoS_2 and 2H-MoS_2. Mater. Chem. Phys. 2012;135:755–761.
[36] Ramakrishna Matte HSS, Gomathi A, Manna A, et al. MoS_2 and WS_2 analogues of graphene. Angew. Chem. Int. Ed. 2010;49:4059–4062.
[37] Kuc A, Zibouche N, Heine T. Influence of quantum confinement on the electronic structure of the transition metal sulfide TS_2. Phys. Rev. B. 2011;83:245213–245216.
[38] Reshak AH, Auluck S. Calculated optical properties of 2H-MoS_2 intercalated with lithium. Phys. Rev. B. 2003;68:125101–125107.
[39] Reshak AH, Auluck S. Band structure and optical response of 2h-MoX_2 compounds (X = S, Se, and Te). Phys. Rev. B. 2005;71:155114–155119.
[40] Ding Y, Wang Y, Ni J, et al. First principles study of structural, vibrational and electronic properties of graphene-like MX_2 (M = Mo, Nb, W, Ta; X = S, Se, Te) monolayers. Physica B. 2011;406:2254–2260.
[41] Johari P, Shenoy VB. Tuning the electronic properties of semiconducting transition metal dichalcogenides by applying mechanical strains. ACS Nano. 2012;6:5449–5456.
[42] Miao Y-P, Ma F, Huang Y-H, et al. Strain effects on electronic states and lattice vibration of monolayer MoS_2. Physica E. 2015;71:1–6.
[43] Zhang W, Zhang P, Su Z, et al. Synthesis and sensor applications of MoS_2-based nanocomposites. Nanoscale. 2015;7:18364–18378.